USGS
science for a changing world

U.S. DEPARTMENT OF THE INTERIOR
U.S. GEOLOGICAL SURVEY

Prepared for the
NATIONAL AERONAUTICS AND SPACE ADMINISTRATION

GEOLOGIC INVESTIGATIONS SERIES I–2684
ATLAS OF VENUS: LAVINIA PLANITIA QUADRANGLE (V–55)

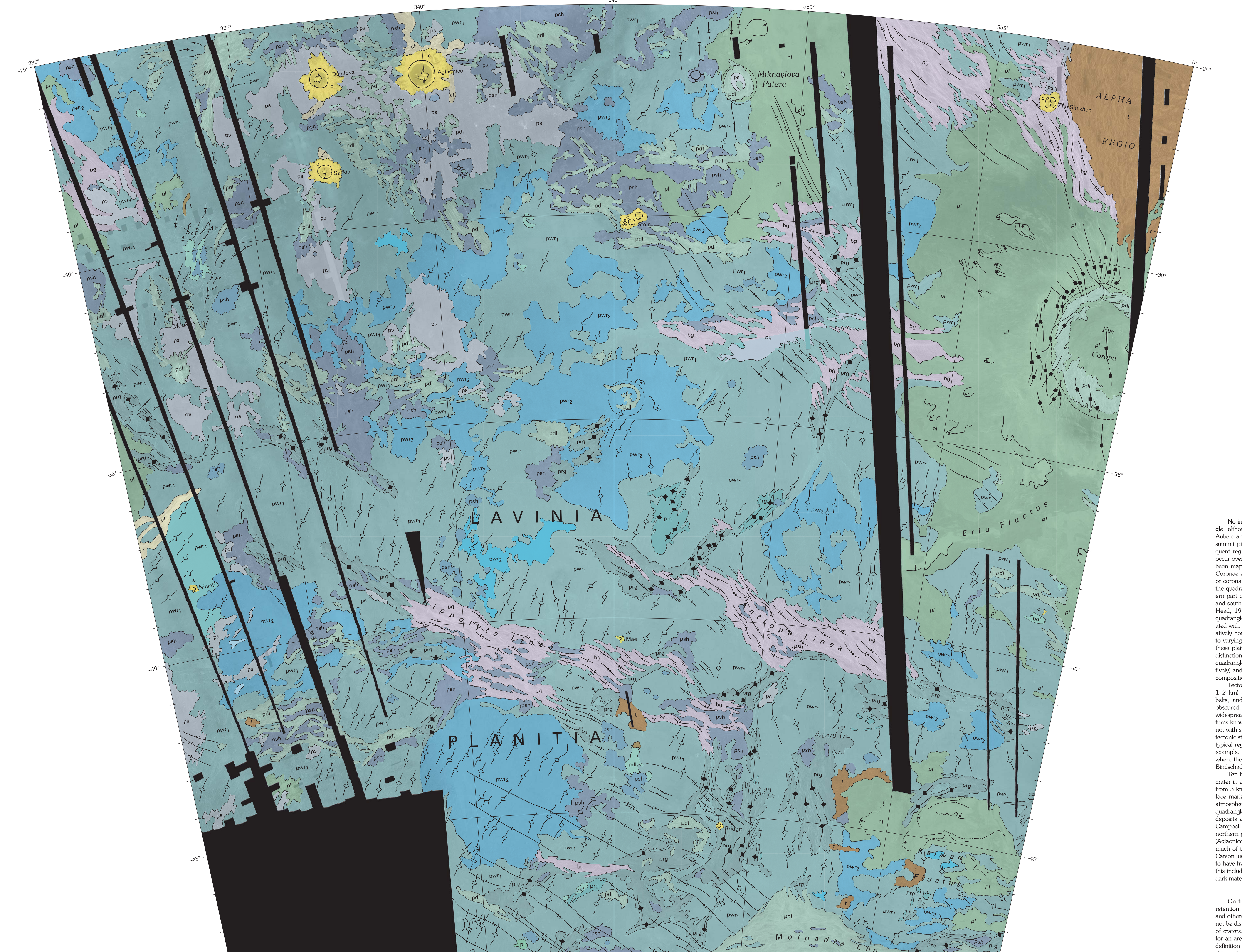

SCALE 1:4 711 886 (1 mm = 4.712 km) AT –25° LATITUDE
1:5 000 000 AT –34° and –73° LATITUDES
LAMBERT PROJECTION

INTERIOR—GEOLOGICAL SURVEY, RESTON, VA—2001

Prepared on behalf of the Planetary Geology Program, Solar System Exploration Division, Office of Space Science, National Aeronautics and Space Administration

Edited by Derrick D. Hirsch; cartography by Ralph O. Aeschliman, Jr. and Darlene A. Casebier

Manuscript approved for publication May 12, 1999

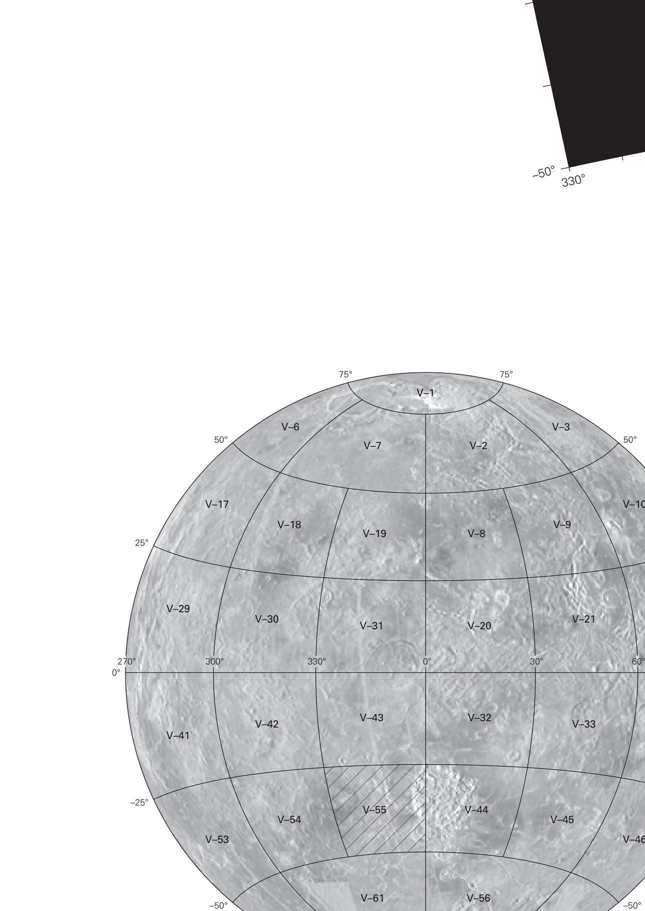

QUADRANGLE LOCATION
Photomosaic location is shown in the western hemisphere of Venus. An outline of 1:5,000,000-scale quadrangles is provided for reference.

CORRELATION OF MAP UNITS

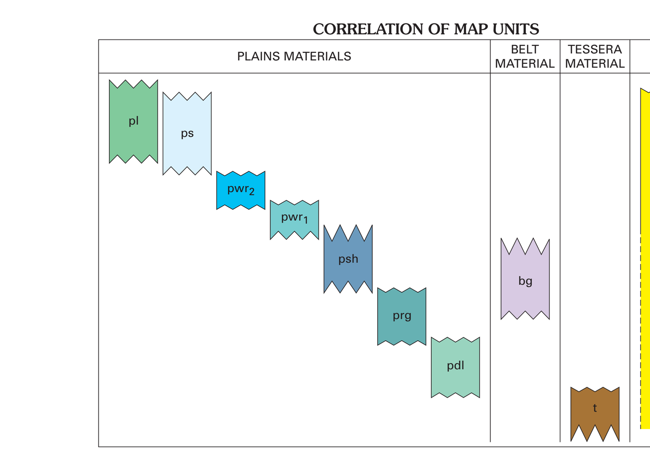

DESCRIPTION OF MAP UNITS

[Map units are defined, characterized, and interpreted on the basis of radar backscatter; surface texture and morphology; associated features of apparent volcanic and tectonic origin; and roughness, reflectivity, emissivity, and topography. Although most map units are rock materials, some are defined on the basis of pervasive tectonic structure that obscures the underlying materials and becomes part of the characteristics of the surface morphology. Type localities are indicated for units previously defined (Basilevsky and Head, 1995b) and reference localities are indicated for units in the quadrangle. Radar properties of the reference areas of each unit are shown in table 1 and the relation between incidence angle and backscatter coefficient for unit type areas is shown in fig. 2]

PLAINS MATERIALS

pl — **Lobate plains material**—Homogeneous plains material with internal elements arranged in parallel to sinuous to lobate radar bright and dark strips and patches; unit boundaries are typically lobate. Type locality: 5.5° N., 196.0° E.; reference locality: 34.39° S., 354.76° E. *Interpretation*: Complexes of lava flows undisturbed by subsequent deformation

ps — **Smooth plains material**—Smooth plains material of uniform, generally low backscatter. Lobate margins common. Type locality: 3.5° N., 198.2° E.; reference locality: 41.76° S., 330.47° E. *Interpretation*: Volcanic plains material unmodified by subsequent deformation

Wrinkle ridged plains material—Homogeneous plains material of intermediate-dark to intermediate-bright radar backscatter complicated by narrow linear to anastomosing wrinkle ridges in parallel lines or intersecting networks. Type locality: 8.0° N., 177.0° E. *Interpretation*: Regional plains material of volcanic origin deformed by wrinkle ridges; sources of plains not obvious. Some small shield-shaped features appear to be kipukas of shield plains material

pwr_2 — **Upper unit**—Plains material of generally high radar backscatter, commonly with lobate boundaries. Embays and is modified by wrinkle ridges. Reference locality: 37.48° S., 350.33° E. *Interpretation*: Lava flows subsequently deformed by wrinkle ridges

pwr_1 — **Lower unit**—Plains material of generally low radar backscatter; commonly mottled locally. Modified by wrinkle ridges. Reference locality: 45.67° S., 350.83° E. *Interpretation*: Lava flows subsequently deformed by wrinkle ridges

psh — **Shield plains material**—Plains material of intermediate radar backscatter characterized by abundant small shield-shaped features (a few up to 10–20 km diameter) commonly with summit pits. Shields occur in clusters, giving unit a locally hilly texture, and as isolated outcrops in relatively smooth plains. Unit commonly occurs on densely lineated plains material; in places crossed by wrinkle ridges. Reference locality: 49.21° S., 342.88° E. *Interpretation*: Shields of volcanic origin; likely the sources of adjacent plains material

prg — **Ridged and grooved plains material**—Characterized by relatively smooth plains having generally densely spaced, sinuous to anastomosing ridges as much as 5–10 km wide and several tens of kilometers long, and some linear grooves, commonly arrayed orthogonally. Formed of preexisting plains whose surfaces contain small shields in places. Arranged in linear belts (100–200 km long and 75–100 km wide). Type locality: 37.7° N., 396.6° E.; reference locality: 46.63° S., 341.89° E. *Interpretation*: Volcanic plains material deformed into ridgelike belts by compression

pdl — **Densely lineated plains material**—Flat plainslike material intensely lineated by closely spaced narrow parallel lineaments 10–20 km long and less than 1 km wide, anastamosing patterns in places; radar bright due to dense fractures. Type locality: 48.5° N., 15.0° E.; reference locality: 48.0° S., 351.5° E. *Interpretation*: Volcanic plains material very highly modified by fractures of probable extensional origin. Local changes in fracture density suggest some resurfacing during formation

BELT MATERIAL

bg — **Groove belt material**—Characterized by numerous short and long curvilinear subparallel lineaments that are typically wide enough to be resolved as fractures and graben. Forms linear belts as much as 500 km long and 150–200 km wide that are characterized by generally high topography but with associated linear depressions. Remnants of preexisting plains can be seen at higher resolution but are not mappable at this scale. Distinguished from densely lineated plains material by lower density and type of fractures and beltlike form. Type locality: 40.60° S., 353.11° E. *Interpretation*: Various materials deformed into broad belts; fractures formed largely by extension

TESSERA MATERIAL

t — **Tessera material**—Radar bright and dominated by closely spaced ridges and grooves oriented in at least two directions, commonly orthogonally; terrain typically elevated. Embayed by plains units. Type locality: 67.5° N., 20.0° E.; reference locality: 25.65° S., 358.92° E. *Interpretation*: Material intensely deformed by compression and extension

CRATER MATERIALS

c — **Undivided crater material**—Craterform material of various diameters including central peaks, floor, walls, rim, and ejecta but lacking dark paraboloid. Reference locality: 26.12° S., 339.67° E. *Interpretation*: Impact crater and associated ejecta that has lost parabola through erosion or formed without one

cf — **Crater flow material**—Characterized by high radar backscatter; lobate margins common. Reference locality: 26.0° S.; 340.5° E. *Interpretation*: Outflows from impact craters

- **Contact**—Dashed where approximately located
- **Ridge**
- **Wrinkle ridge**
- **Furrow**
- **Sharp groove**
- **Subdued groove**
- **Lava flow front**—Arrow indicates flow direction
- **Lava channel**
- **Steep-sided dome**
- **Corona**
- **Rim of impact crater (>10 km diameter)**
- **Central peak of impact crater**
- **Rim of impact crater (<10 km diameter)**
- **Depression**

The Magellan Mission

The Magellan spacecraft orbited Venus from August 10, 1990, until it plunged into the venusian atmosphere on October 12, 1994. Magellan had the objectives of (1) improving knowledge of the geologic processes, surface properties, and geologic history of Venus by analysis of surface radar characteristics, topography, and morphology and (2) improving knowledge of the geophysics of Venus by analysis of venusian gravity.

The Magellan spacecraft carried a 12.6-cm radar system to map the surface of Venus. The transmitter and receiver systems were used to collect three datasets: synthetic aperture radar (SAR) images of the surface, passive microwave thermal emission observations, and measurements of the backscattered power at small angles of incidence, which were processed to yield altimetric data. Radar imaging and altimetric and radiometric mapping of the venusian surface were done in mission cycles 1, 2, and 3, from September 1990 until September 1992. Ninety-eight percent of the surface was mapped with radar resolution of approximately 120 meters. The SAR observations were projected to a 75-m nominal horizontal resolution; these full-resolution data compose the image base used in geologic mapping. The primary polarization mode was horizontal-transmit, horizontal-receive (HH), but additional data for selected areas were collected for the vertical polarization sense. Incidence angles varied from about 20° to 45°.

High-resolution Doppler tracking of the spacecraft was done from September 1992 through October 1994 (mission cycles 4, 5, 6). High-resolution gravity observations from about 950 orbits were obtained between September 1992 and May 1993, while Magellan was in an elliptical orbit with a periapsis near 175 kilometers and an apoapsis near 8,000 kilometers. Observations from an additional 1,500 orbits were obtained following orbit-circularization in mid-1993. These data exist as a 75° by 75° harmonic field.

Magellan Radar Data

Radar backscatter power is determined by the morphology of the surface at a broad range of scales and by the intrinsic reflectivity, or dielectric constant, of the material. Topography at scales of several meters and larger can produce quasi-specular echoes, with the strength of the return greatest when the local surface is perpendicular to the incident beam. This type of scattering is most important at very small angles of incidence, because natural surfaces generally have few large tilted facets at high angles. The exception is in areas of steep slopes, such as ridges or rift zones, where favorably tilted terrain can produce very bright signatures in the radar image. For most other areas, diffuse echoes from roughness at scales comparable to the radar wavelength are responsible for variations in the SAR return. In either case, the echo strength is also modulated by the reflectivity of the surface material. The density of the upper few wavelengths of the surface can have a significant effect. Low-density layers, such as crater ejecta or volcanic ash, can absorb the incident energy and produce a lower observed echo. On Venus, a rapid increase in reflectivity exists at a certain critical elevation, above which high-dielectric minerals or coatings are thermodynamically stable. This effect leads to very bright SAR echoes from virtually all areas above that critical elevation.

The measurements of passive thermal emission from Venus, though of much lower spatial resolution than the SAR data, are more sensitive to changes in the dielectric constant of the surface than to roughness. As such, they can be used to augment studies of the surface and to discriminate between roughness and reflectivity effects. Observations of the near-nadir backscatter power, collected using a separate smaller antenna on the spacecraft, were modeled using the Hagfors expression for echoes from gently undulating surfaces to yield estimates of planetary radius, Fresnel reflectivity, and root-mean-square (rms) slope. The topography data produced by this technique have horizontal footprint sizes of about 10 km near periapsis and a vertical resolution of approximately 100 m. The Fresnel reflectivity data provide a comparison to the emissivity maps, and the rms slope parameter is an indicator of the surface tilts, which contribute to the quasi-specular scattering component.

INTRODUCTION

The Lavinia Planitia quadrangle (V–55) is in the southern hemisphere of Venus and extends from 25° to 50° south latitude and from 330° to 360° longitude. It covers the central and northern part of Lavinia Planitia and parts of its margins. Lavinia Planitia consists of a centralized deformed lowland flooded by volcanic deposits and surrounded by Dione Regio to the west (Keddie and Head, 1995), Alpha Regio tessera (Bindschadler and others, 1992a) and Eve Corona (Stofan and others, 1992) to the northeast, an extensive rift zone and coronae belt to the east and south (Baer and others, 1994; Magee and Head, 1995), Mylitta Fluctus to the south (Magee Roberts and others, 1992), and Helen Planitia to the southwest (Senske and others, 1991). In contrast to more elongated lowland areas on Venus, the Lavinia Planitia area is one of several large, relatively equidimensional lowlands (basins) and as such is an important region for the analysis of processes of basin formation and volcanic flooding.

Before the Magellan mission, Lavinia Planitia was known on the basis of Pioneer–Venus altimetry to be a lowland area (Pettengill and others, 1980); Arecibo radar images showed that it was surrounded by several coronalike features and riftlike fractures parallel to the basin margin to the east and south (Senske and others, 1991; Campbell and others, 1990). Arecibo data further revealed that the interior contained complex patterns of deformational features in the form of belts and volcanic plains, and several regions along the margins were seen to be the sources of extensive outpourings of digitate lava flows into the interior (Senske and others, 1991; Campbell and others, 1990). Early Magellan results showed that the ridge belts are composed of complex deformational structures of both extensional and contractional origin (Squyres and others, 1992; Solomon and others, 1992) and that the complex lava flows (fluctus) along the margins (Magee Roberts and others, 1992) emanated from a variety of sources ranging from volcanoes to coronae (Magee and Head, 1995; Keddie and Head, 1995). In addition, global analysis of the distribution of volcanic features revealed that Lavinia Planitia is an area deficient in the distribution of distinctive volcanic sources and coronalike features (Head and others, 1992; Crumpler and others, 1993). Lavinia Planitia gravity and geoid data show that the lowland is characterized by a −30 mGal gravity anomaly and a −10 m geoid anomaly, centered on eastern Lavinia (Bindschadler and others, 1992b; Konopliv and Sjogren, 1994). Indeed, the characteristics and configuration of Lavinia Planitia have been cited as evidence for the region being the site of large-scale mantle downwelling (Bindschadler and others, 1992b). Thus, this region is a laboratory for the study of the formation of lowlands, the emplacement of volcanic plains, the formation of associated tectonic features, and their relation to mantle processes. These questions and issues are the basis for our geologic mapping analysis.

In our analysis we have focused on the geologic mapping of the Lavinia Planitia quadrangle using traditional methods of geologic unit definition and characterization for the Earth (for example, American Commission on Stratigraphic Nomenclature, 1961) and planets (for example, Wilhelms, 1990) appropriately modified for radar data (Tanaka, 1994). We defined units and mapped key relations using the full resolution Magellan synthetic aperature radar (SAR) data (mosaicked full resolution basic image data records, C1–MIDR's, F-MIDR's, and F-Maps) and transferred these results to the base map compiled at a scale of 1:5 million. In addition to the SAR image data, we incorporated into our analyses digital versions of Magellan altimetry, emissivity, Fresnel reflectivity, and roughness data (root mean square, rms, slope). The background for our unit definition and characterization is described in Tanaka (1994), Basilevsky and Head (1995a, b), and Basilevsky and others (1996).

MAGELLAN SAR AND RELATED DATA

The synthetic aperture radar (SAR) instrument (12.6 cm, S-band) flown on the Magellan spacecraft provided the image data used in this mapping and interpretation. SAR images are a record of the echo (radar energy returned to the antenna), which is influenced by surface composition, slope, and wavelength-scale surface roughness. Viewing and illumination geometry also will influence the appearance of surface features in SAR images. Guidelines for geologic mapping using Magellan SAR images and detailed background to aid in their interpretation can be found in Elachi (1987), Saunders and others (1992), Ford and Pettengill (1992), Tyler and others (1992), and Tanaka (1994). In the area of the Lavinia Planitia quadrangle, incidence angles are such that backscatter is dominated by variations in surface roughness at wavelength scales. Rough surfaces appear relatively bright, whereas smooth surfaces appear relatively dark. Variations also occur depending on the orientation of features relative to the incident radiation (illumination direction), with features normal to the illumination direction being more prominent than those oriented parallel to it. Full-resolution images have a pixel size of 75 m; C1–MIDR's contain the SAR data displayed at ~225 m/pixel. Altimetry data and stereo images were of extreme importance in establishing geologic and stratigraphic relations between units. Also essential in the analysis of the geology of the surface are data obtained by Magellan on the emissivity (passive thermal radiation), reflectivity (surface electrical properties), and rms slope (distribution of radar wavelength-scale slopes). Aspects of these measurements were used in unit characterization and interpretation; background on the characterstics of these data and their interpretation can be found in Saunders and others (1992), Ford and Pettengill (1992), Tyler and others (1992), Tanaka (1994), and Campbell (1995).

GENERAL GEOLOGY

Several different geologic processes have influenced the Lavinia Planitia region and have combined together to form its geologic record. Volcanism is the dominant process of crustal formation on Venus (Head and others, 1992) and production of the observed geologic units in this map area. Tectonic activity has modified some of these basic crustal materials (for example, Solomon and others, 1992; Squyres and others, 1992) in a variety of modes (extension, contraction, and shear), and in places deformation is so extensive, as in the case of tessera terrain, that the deformational features become part of the definition of the material unit (see also Tanaka, 1994; Scott and Tanaka, 1986). Impact cratering also has locally influenced regions in the quadrangle, most notably in the area dominated by Danilova, Saskia, and Aglaonice craters, but in general has not been an influential process over the quadrangle as a whole. Eolian processes require a source of sediment to produce deposits and thus are concentrated around impact craters and localized around tectonic fractures and scarps (for example, Greeley and others, 1992).

No intermediate to large volcanic edifices (Head and others, 1992) are observed in the quadrangle, although small shield volcanoes less than about 15 km diameter (Guest and others, 1992; Aubele and Slyuta, 1990) are common. The small shields are low in elevation, commonly have a summit pit, do not appear to have distinct associated flows, and are commonly embayed by subsequent regional plains deposits. Although not continuous, concentrations of small shield volcanoes occur over all parts of the quadrangle. Three steep-sided domes (Pavri and others, 1992; fig. 1) have been mapped and are found in stratigraphic association with the abundant small shield volcanoes. Coronae are not well-developed or abundant in the lowlands of Lavinia Planitia, but three coronae or coronalike features are seen (fig. 1), predominantly in the northern topographically higher part of the quadrangle. The 330-km-diameter Eve Corona (32.0° S., 359° E.) is exposed in the northeastern part of the quadrangle and is one of several arrayed along the margins of the basin to the east and south, but outside the map area (Stofan and others, 1992; Baer and others, 1994; Magee and Head, 1995). Extensive lobate lava flows, the fluctus, emanate from these features and enter the quadrangle from the margins. Other lobate lava flows enter the quadrangle from the edifices associated with Dione Regio to the west and a corona to the north. Most of the quadrangle comprises relatively homogeneous plains interpreted to be of volcanic origin, and modified by tectonic structures to varying, but usually low, degrees. The source vents for these plains are not well known. Some of these plains display radar backscatter variations and apparent flow fronts that permit stratigraphic distinctions among subunits. The composition of these volcanic plains is not known from data in this quadrangle although Venera 9 and 10 (northeastern and southeastern slope of Beta Regio respectively) and Vega 2 (Rusalka Planitia) lander geochemical analyses of sites in similar terrains suggest compositions similar to terrestrial tholeiitic basalt (Basilevsky and others, 1992).

Tectonic features in the Lavinia Planitia quadrangle include individual narrow (less than about 1–2 km) graben hundreds of kilometers in length, concentrations of parallel narrow graben into belts, and some concentrations in such high density that the underlying terrain is completely obscured. Compressional deformation is manifested as wrinkle ridges (anticlines and thrust faults), widespread throughout the plains, and as various large amplitude and long wavelength fold structures known as arches and ridge belts. Evidence for shear also exists within the quadrangle, although not with significant strike-slip offset (for example, Squyres and others, 1992). In some places, several tectonic styles have operated together or in sequence to produce terrain more heavily deformed than typical regional plains. The annulus around Eve Corona, where fractures and graben coexist, is an example. The most extreme example is in Alpha Regio in the northeastern part of the quadrangle where the deformation is so intense that it becomes a major part of the unit definition (for example, Bindschadler and others, 1992a).

Ten impact craters, one impact crater cluster, and the lobate outflow deposits associated with a crater in adjacent Dione Regio are mapped in the quadrangle (fig. 1). The craters range in diameter from 3 km, through 10–15 km for the cluster, to 63 km for crater Aglaonice. Three splotches (surface markings and deposits interpreted to be formed from airblasts from projectiles traversing the atmosphere; for example, Schaber and others, 1992; Ivanov and others, 1992) were detected in the quadrangle (fig. 1). Extended surface deposits emplaced during the cratering event (both outflow deposits and remnants of dark parabolas; Schaber and others, 1992; Phillips and others, 1992; Campbell and others, 1992; Schultz, 1992) were noted and are particularly concentrated in the northern part of the quadrangle where three craters are found within less than 300 km of each other (Aglaonice, 63 km diameter; Danilova, 49 km diameter; Saskia, 37 km diameter). The origin of much of the dark material appears to be primarily parts of the parabola associated with the crater Carson just to the north (Bender and others, 1999). This same area is the main region that appears to have fragmental surface materials which have been redistributed by eolian processes. Evidence for this includes wind streaks oriented east-west, particularly north of Aglaonice, and diffuse patches of dark material.

STRATIGRAPHY

On the basis of an analysis of the global size-frequency distribution of impact craters, a crater retention age of 500 Ma (Schaber and others, 1992; Phillips and others, 1992) or 300 Ma (Strom and others, 1994) for the present surface of Venus was proposed. The crater areal distribution cannot be distinguished from a spatially random population, which, together with the small total number of craters, means that crater size-frequency distributions cannot be used to date stratigraphic units for an area the size of the Lavinia Planitia quadrangle. Therefore, attention must be focused on the definition of geologic units and structures and on analysis of crosscutting, embayment, and superposition relations among structures and units in order to establish the regional geologic history.

Although we have mapped tectonic structure independent of geologic units, in many cases tectonic features are such a pervasive part of the morphology of the terrain that it becomes part of the definition of a unit. For example, our tessera unit is similar to several members of the Olympus Mons Formation (Aureole members 1–4), which are defined on the basis of tectonic structure ("...corrugated, cut by numerous faults that formed scarps and deep troughs and grabens." [Scott and Tanaka, 1986]). Our plains unit with wrinkle ridges is analogous to Member 1 of the Arcadia Formation on Mars ("...low-lying plains... Mare-type (wrinkle) ridges common." [Scott and Tanaka, 1986]). In other cases, the approach depends on scale and density. For example, where the structures are more discrete and separated, we map them separately and not as a specific unit, whereas in other cases, where they are very dense and tend to obscure the underlying terrain, we choose to map them as a unit. Here we summarize the stratigraphic units and structures and their relations.

The unit interpreted to be stratigraphically oldest in the quadrangle is tessera material (unit t), which is embayed by most of the other units within this quadrangle. Tessera terrain is radar bright, consists of at least two sets of intersecting ridges and grooves, and is a result of tectonic deformation of some precursor terrain (Barsukov and others, 1986; Basilevsky and others, 1986; Bindschadler and Head, 1991; Sukhanov, 1992; sometimes referred to as complex ridged terrain, Solomon and others, 1992). Arches, ridges, grooves, and graben are tectonic features, so structure is an essential component of the tessera terrain and a key aspect of the unit definition, similar to the situation in the Aureole members of the Olympus Mons Formation (Scott and Tanaka, 1986). Globally, tessera material occupies about 8% of the surface of Venus (Ivanov and Head, 1996) and occurs as large blocks and small islands standing above and embayed by adjacent plains. These types of occurrences are mirrored in this quadrangle, where the southwestern portion of a large tessera block about 1,300 km acoss is exposed (Alpha Regio), and several small patches are seen in the southern part of the quadrangle. In the portion of Alpha Regio exposed in this quadrangle, the westernmost margin is characterized by north-south-trending structures and the inner portion by more complex deformation patterns (see also Bindschadler and others, 1992a; Gilmore and Head, 1992).

Many plains units dominate the quadrangle. The stratigraphically oldest plains unit is densely lineated plains material (unit pdl), which is characterized by relatively flat surfaces on a regional scale and by swarms of parallel and subparallel lineaments (resolved as fractures if they are wide enough) having typical spacing of less than 1 km. Although the unmodified precursor terrain for the densely lineated plains material is not observed, the flatness suggests that it was plains. Although fractures are structural elements, they are such a pervasive part of the morphology of this terrain that it becomes a key aspect of the definition of the unit, as in several of the Mars examples cited above. Densely lineated plains are distributed relatively evenly throughout the quadrangle in small patches and linear ridges, in close association with ridge belts and groove belts.

Following the emplacement and deformation of densely lineated plains, a plains material of relatively high radar albedo was emplaced. This unit, ridged and grooved plains material (unit prg), is commonly deformed by relatively broad (5–10 km wide) ridges tens of kilometers long, typically arranged en echelon, and by orthogonal grooves and graben, which tend to postdate the ridges and arches. This unit is arranged in linear outcrops or belts 75–100 km wide and 100–200 km long and is largely equivalent to the ridge belts of Squyres and others (1992). These belts are formed from preexisting relatively flat plains. Ridged and grooved plains are interpreted to be volcanic plains materials deformed into ridgelike belts by compression. Ridged and grooved plains occur primarily in the southeastern part of the quadrangle, but some occurrences extend toward Dione Regio (east of the map area). Occurrences are oriented predominantly northeast-southwest, but near Dione occurrences of the unit strike northwest-southeast.

After the formation of ridged and grooved plains and their deformation into ridges and broad arches, swarms of narrow grooves were formed. In some cases, grooves are so closely spaced that they tend to obscure underlying terrain and their presence takes on a defining character to the terrain. These concentrations are characterized by numerous short and long curvilinear subparallel lineaments that are commonly wide enough to be resolved as fractures and graben. These occurrences form linear belts (groove belt material, unit bg) as much as 500 km long and 150–200 km wide that are characterized by generally high topography but with associated linear depressions. In detailed mapping at the F-Map scale, remnants of preexisting plains can be seen. Orientations of grooves in groove belts are shown within the unit and generally trend northwest-southeast, parallel to the trend of the groove belts as a whole. Groove belts are concentrated in the central and east-central part of the quadrangle.

Following the emplacement of ridged and grooved plains and the tectonic episode forming groove belts, shield plains material (unit psh) of intermediate radar albedo was emplaced. This unit is characterized by abundant small shield-shaped features ranging from a few kilometers in diameter up to about 10–20 km, commonly with summit pits. Although small clusters of shields were recognized earlier planetwide (Head and others, 1992), they were thought to be localized occurrences possibly related to individual sources such as hot spots. Later work in Vellamo Planitia (Aubele, 1994, 1995) recognized that many of these occurrences represented a stratigraphic unit in this region, and subsequently this unit has been recognized in many areas on the planet (Basilevsky and Head, 1995b; Basilevsky and others, 1997), including this quadrangle. Shields characterizing this unit occur in clusters, giving the unit a locally hilly texture, and as isolated outcrops in relatively smooth plains. The shields are interpreted to be of volcanic origin and are likely to be the sources of the adjacent smooth plains, although specific flow units associated with the shields have not been identified. The unit is widely distributed in the quadrangle except along the eastern margin, where it is likely buried by younger plains units, particularly those associated with the young digitate flows emanating from the basin margins (Magee and Head, 1995). Some isolated occurrences of shields occur where subsequent plains units embay shield plains and form kipukas (flooding the bases of the shields and leaving the tops exposed). As the radar brightness of the two units commonly is different, this permits an estimate to be made of the thickness (about 100–200 m) of the margins of the embaying unit, since information exists on the topography of the shields (Guest and others, 1992).

After the emplacement of these earlier plains units (and locally the formation of groove belts; see following section), the most widespread plains unit in the quadrangle, wrinkle ridged plains material, was emplaced. This unit comprises morphologically smooth, homogeneous plains material of intermediate-dark to intermediate-bright radar albedo complicated by narrow linear to anastomosing wrinkle ridges (a structural element) in parallel lines or intersecting networks. [This unit is analogous to ridged plains material on Mars (Scott and Tanaka, 1986), which is defined by "long, parallel, linear to sinuous mare-type (wrinkle) ridges."] In the map area, the wrinkle ridges typically are less than 1 km wide and a few tens of kilometers long; in some areas they may be smaller, whereas in others they are larger. Their trend often varies locally even within one site, but in the Lavinia Planitia area they are dominated by a north-northeast sweeping trend extending from the south to the north in the quadrangle. The unit is interpreted to be regional plains of volcanic origin that were subsequently deformed by wrinkle ridges, in some cases during emplacement of the unit as a whole. Volcanic edifices, channels, and sources of the plains are not obvious, although some small shield-shaped features appear to be kipukas of shield plains material (unit psh). Wrinkle ridged plains material is divided into two units. The lower unit (unit pwr_1) generally has a relatively low radar albedo but can be mottled locally. The upper unit (unit pwr_2) generally has a relatively high radar albedo and lobate boundaries. Together these two units form more than 60% of the surface of the quadrangle and occur predominantly in low-lying regions between linear highs composed of preexisting units, ridge belts, and fracture belts (for example, Antiope, Hippolyta, and Molpadia Lineae). Unit pwr_1 is the most widespread of the two units, and unit pwr_2 forms less than about 30% of the combined area of the two units, apparently largely covering unit pwr_1, primarily in the central part of the quadrangle.

The youngest plains units in the stratigraphic sequence are characterized by distinctive lobate and digitate shapes and margins, and morphologically smooth surfaces commonly unmodified by wrinkle ridges or other structural elements. Two types are recognized: smooth plains material (unit ps) of uniform, generally low albedo, and lobate plains material (unit pl) having internal elements arranged in parallel to sinuous to lobate radar bright and dark strips and patches, and unit boundaries that are typically lobate. Both of these units are interpreted as complexes of lava flows undisturbed by subsequent deformation. In the Lavinia Planitia quadrangle, smooth plains material occurs predominantly in small patches along the west margin, related to the flanks of Dione Regio, and at the north edge of the quadrangle; lobate plains material occurs predominantly along the east margin of the basin in the form of the large flow deposits (for example, Eriu and Kaiwan Fluctus) emanating from the coronae and volcanoes along the margin of the basin.

Impact craters and related deposits are observed in several places in the quadrangle (fig. 1). [On the map they are separated into undivided crater material (unit c) and proximal textured and outflow deposits (unit cf), which lack the distal dark paraboloid.] Several craters are characterized by a surrounding of radar dark material that partly to wholly obscures the underlying terrain, which appears to be a dark paraboloid originating from the impact crater Carson to the north (Bender and others, 1999). Carson is interpreted to be an impact crater with an annulus of fine-grained airfall ejecta (for example, Schultz, 1992; Campbell and others, 1992). We observed only one crater in the quadrangle that may be embayed by lava flows (37.85° S., 359.05° E.; 3.0 km diameter; possibly embayed by flows of the lower unit of wrinkle ridged plains material) and only one crater that is possibly cut by tectonic features (48.80° S., 354.95° E.; 4.5 km diameter; possibly cut by unit pdl, fractures related to densely lineated plains).

Some surficial streaks and patches of apparently unconsolidated material that has been redistributed by eolian processes (for example, Greeley and others, 1992) are observed in the quadrangle but are not mapped as a specific unit. They are primarily in the north-central region, where material from the crater Carson has been partially redistributed.

STRUCTURES

Various tectonic features are observed and mapped in the quadrangle. Long linear fractures and some paired and facing scarps interpreted to be graben are seen in the eastern part of the quadrangle. They are 150–700 km long, oriented northwest-southeast, and are spaced 30–150 km apart, cutting virtually all stratigraphic units. In some cases, graben are so closely spaced that they tend to obscure underlying terrain and their presence takes on a defining character to the terrain.

Concentrations of graben (unit bg) are distinguished from densely lineated plains (unit pdl) by their beltlike form, a lower density of tectonic features, and the character of the fractures (more distinctly recognizable graben in unit bg). Groove belts appear to be distinctive stratigraphically. The structure of the belts crosscuts material of ridged and grooved plains and other older units and, in turn, are embayed mostly by shield plains and wrinkle ridged plains material. Some of the structures of groove belts cut the surface of these latest units. The individual fractures cutting many younger units and mapped as separate structures commonly are oriented in the same direction and may represent the waning stages of continued deformation.

Several types and scales of features of compressional origin also are observed. Wrinkle ridges are seen throughout the quadrangle and are so important in the broad plains that they in part define and characterize wrinkle ridged plains material. These features are mapped in a representative sense in terms of density and trend by individual wrinkle ridge symbols. Ridged and grooved plains (unit prg) are dominated by ridges and arches, and the general trends of these also are represented in the units by symbols. Ridged and grooved plains form predominantly north-northeast- and northeast-trending bands or belts that are largely equivalent to the ridge belts of Squyres and others (1992). Basilevsky and Head (1995a, b) described a structure (ridge belts, RB) that was a belt consisting of a cluster of densely spaced ridges 5–10 km wide and a few tens of kilometers long; this unit was often transitional to ridged and grooved plains (unit prg). Although we did not map ridge belts in this area, the belts of ridged and grooved plains are closely related.

No major volcanic edifices exist wholly within the Lavinia Planitia quadrangle, although several coronae are seen (fig. 1), the largest of which is the 330-km-diameter Eve at the east margin of the map area. This structure is part of a chain that extends along the east and south margins of Lavinia Planitia (Baer and others, 1994; Magee and Head, 1995). Eve Corona is defined by an annulus of highly fractured and intensely deformed terrain that is very similar to densely lineated plains, although it is not completely clear if it is temporally correlated with this unit elsewhere in the map area because of lack of continuous outcrop. The corona is also characterized by concentric and radial graben and fractures both inside and along the margins of the annulus, which are individually mapped. The corona is surrounded by an extensive apron of flows of lobate plains (unit pl). Other coronae and coronalike features often have an annulus made up of material resembling densely lineated plains broadly embayed by younger plains units (Basilevsky and Head, 1998; Ivanov and Head, 1998). The northernmost corona (26.8° S., 348.3° E. [referred to as Mikhaylova Patera by the International Astronomical Union, 1999]) is embayed by flows of lobate plains, some of which appear to emanate from the corona. The corona in the central part of the map area (34.5° S., 345.4° E.) is surrounded by a deposit of the upper unit of wrinkle ridged plains material and is probably the source of this unit. The two coronalike features in the western part of the map area (28.4° S., 331.2° E.; 31.5° S., 332.2° E. [referred to as Cipactli Mons by the International Astronomical Union, 1999]) have smooth plains associated with the flooding of their interiors and portions of their exteriors. On the basis of these data, the structural deformation of the coronae apparently occurred early, but that volcanism continued in several of them until relatively recent times.

GEOLOGIC HISTORY

The Lavinia Planitia area is one of the several large relatively equidimensional lowland areas of Venus and is an important region for analysis of processes of lowland formation and volcanic flooding. Major questions include: What is the sequence of events in the formation and evolution of large-scale equidimensional basins on Venus? What are the characteristics of the marginal areas surrounding these basins? How do the units and implied geologic histories in both the basin and the marginal areas compare within Lavinia? When did the Lavinia Planitia basin and its marginal region form and is there any evidence that the basin represents a stage in the evolution of other terrain types, such as tessera? How do the units in Lavinia Planitia compare with each other and what information do they provide concerning models for Venus global stratigraphy and tectonic history? Here we discuss stratigraphic positions of units, their temporal correlations, and the implied geologic history of the region. We also examine the sequence of tectonic deformation and its interpretation as well as the evolution of volcanic styles. We conclude with an assessment of the geologic history of Lavinia Planitia in relation to models for the global evolution of Venus.

The stratigraphically oldest unit in the map area is the tessera, a high-standing complexly deformed unit of which the largest outcrop is exposed in Alpha Regio. Tessera is consistently embayed by younger plains material of apparent volcanic origin. Consistent with observations made on regional (Bindschadler and others, 1992a) and global scales (Ivanov and Head, 1996), tessera material in Alpha Regio was formed from some precursor material that was initially deformed by shortening, folding, and shear, which produced more highly deformed terrain than seen in any subsequent units on Venus, and then underwent extensional deformation (cut by graben of various types) to produce the generally orthogonal structural fabric typical of much of the tessera planetwide. The principal massif of Alpha tessera shows chaotically organized broad ridges several tens of kilometers across cut by numerous narrow and shallow graben that are mostly orthogonal to the ridges. At the west margin of Alpha Regio, a north-south-trending band of tessera is dominated by linear structure having fewer orthogonal features that also predate subsequent units. Other smaller outcrops are exposed as kipukas in the quadrangle, and on the basis of this distribution and the global distribution of similar small outliers, tessera terrain is thought to exist extensively in the subsurface beneath younger plains units. Whether this distribution is planetwide or whether some other unit might be laterally equivalent to the tessera is unclear. No direct evidence exists in the map area for the duration of the formation with the characteristic structural pattern of tessera, but global crater studies (Ivanov and Basilevsky, 1993; Gilmore and others, 1996) suggest that it was of relatively short duration (for example, tens of millions of years).

Marginal to the tessera terrain and embaying it are plains that have been densely fractured (unit pdl) and in some cases have a structural fabric orientation similar to the latest phase of deformation in tessera (for example, Basilevsky and Head, 1995a, fig. 4). The deformation patterns are very dense and unidirectional (in contrast to the orthogonal patterns of the tessera), but both extension and shear are evident. This unit is interpreted to be volcanic plains that embayed early tessera, but which were deformed by the latest phases of tessera deformation. Densely lineated plains are thus partly laterally equivalent to tessera, and the west margin of Alpha Regio is an example of such a transition (Gilmore and Head, 1992). Densely lineated plains material makes up a small percentage of the surface outcrop but is widespread in the map area, suggesting more extensive presence in the subsurface.

Following the emplacement and deformation of densely lineated plains material (unit pdl), a less intensely deformed plains unit was emplaced (ridged and grooved plains material, unit prg). Although little evidence exists for sources, the smooth surface texture of the background material of the unit strongly suggests that it is of volcanic origin. The most important features of ridged and grooved plains are ridges (commonly curvilinear arches 5–10 km wide and comparable to lunar mare arches of compressional origin) and less numerous fractures (typically graben a few kilometers across) which are very pervasive from place to place. Features of contractional and extensional origin are commonly orthogonally arrayed, with the fractures and graben tending to cut the ridges and arches. The unit occurs as broad arches (as much as 100–150 km across) striking northeast-southwest in the central part of the map area and northwest-southeast in the western and eastern parts. The parallelism of the strike of the tectonic features and broad arches of this unit suggests that the deformation that produced the tectonic features is also similar to that which produced the arches. Thus, the period during which this unit was formed was characterized by emplacement of widespread volcanic plains and their subsequent deformation into broad arches with distinctive ridges and fractures. On the basis of its present topographic configuration, this unit and its deformation appear to have produced the second-order topography of the basin, that is, broad segmentation into local low regions defined by linear and anastomosing arches of ridged and grooved plains standing several hundred meters above the surrounding terrain.

After the formation of ridged and grooved plains and their deformation into ridges and broad arches, swarms of narrow (as much as a few kilometers across) graben were formed, and these are observed today as broad beltlike regions known as groove belts (Squyres and others, 1992). Groove belts are a few hundred kilometers wide and hundreds of kilometers long and are oriented northwest-southeast where they are exposed, which is predominantly in the central and northern parts of the map area. Topographically the groove belts represent local highs with many circular, equidimensional, and elongate (in some places almond-shape) depressions within them. Formation of the belts of graben marks an episode of extension that was generally uniformly oriented and apparently unevenly distributed throughout Lavinia Planitia. Groove belts are transitional with some of the fractures in ridged and grooved plains and appear to cut some portions of shield plains, yet shield plains (unit psh) are seen embaying groove belts and forming in the depressions within the groove belts.

Following emplacement and deformation of ridged and grooved plains and the episode of groove belt formation, another distinctly different plains unit (shield plains material, unit psh) was emplaced in many parts of the map area and is now preserved as extensive occurrences along the margins of the deformation belts of ridged and grooved plains (or as isolated occurrences within them) and as patches between the belts in relatively high areas. The abundant shield volcanoes and intershield plains that are characteristic of this unit are noticeably different from the volcanic style of both ridged and grooved plains and subsequent plains with wrinkle ridges. The extent of these vents indicates widespread local and shallow magma sources during the emplacement of shield plains. The close association of this unit with groove belts suggests that the widespread shields may be related to extensional deformation at least locally. The shield plains material embays ridged and grooved plains material, but on the basis of the outcrop patterns of subsequent units (wrinkle ridged plains material) unit psh underwent some tilting after its emplacement. The symmetry of the shields suggests that the slopes were flat at the time of emplacement. The lack of extensive development of deformational features demonstrates that regional deformation had further waned in intensity.

Subsequent to the emplacement of shield plains material and its continued downwarping and tilting, the style of volcanism changed. Instead of abundant small shield volcanoes, broad units of plains, now regionally deformed by wrinkle ridges (units pwr_1 and pwr_2), were emplaced from sources that are now rarely visible. The presence of sinuous channels (in Lavinia outside the map area, and elsewhere; Basilevsky and Head, 1996) and the wide extent of these units suggest emplacement in high-effusion-rate eruptions from a few sources, in distinct contrast to the widespread and abundant shield volcanoes just preceding this phase. On the basis of the outcrop distribution and the isolation of several of the basins, the sources were distributed in different parts of the map area and may have fed individual deposits in small basins.

At least one occurrence of unit pwr_2 may have originated from a corona in the central part of the map area, and several other occurrences of this unit along the east margin adjacent to and underlying later flows of lobate plains (unit pl) suggest that regional deposition of the lower unit of wrinkle ridged plains material (unit pwr_1) may have given way to deposits of the upper unit, which was associated with specific sources such as coronae. Deposits of wrinkle ridged plains material cover well over one-half of the map area and are concentrated in the lowland areas between fracture belts and belts of ridged and grooved plains. Their distribution is good evidence that most of the topography observed today was formed prior to the emplacement of the majority of wrinkle ridged plains material. However, the volcanic plains of units pwr_1 and pwr_2 were further deformed by the formation of wrinkle ridges during and subsequent to their emplacement; the central parts of deposits of these units are depressed up to a few hundred meters from surrounding marginal deposits of the same unit. Wrinkle ridges are oriented in a north-northeast to south-southwest direction, generally consistent with the tectonic fabric and principle stress directions typical of ridged and grooved plains. Thus, the deformation recorded in units prg, pwr_1, and pwr_2 appears to be relatively consistent in structural trends but reflects a decrease in the intensity of shortening and deformation with time. In a few cases some smooth lava flows (unit ps) similar to the underlying plains (units pwr_1 and pwr_2) were emplaced in the western and northern portions of the basin and are apparently unmodified by wrinkle ridges.

Near the end of emplacement of wrinkle ridged plains material, extensive lobate and digitate flows (unit pl) originated from coronae and volcanoes along the margins of the Lavinia Planitia basin and flowed down the slopes into the basin. The only source in the map area is Eve Corona, from which numerous flows emanate and extend down into the basin, following preexisting topography. Only very locally are flows of this type deformed by wrinkle ridges, which suggests that they are either very recent and as yet undeformed or that wrinkle ridge deformation as a general phenomena ceased by this time. On the basis of the general decrease in tectonic deformation intensity as a function of time, we interpret the general absence of wrinkle ridges in lobate plains to be the result of waning deformational forces. Despite the fact that these are the youngest flows in the map area, evidence from Eve and other coronae indicate that coronae interiors and margins contain units equivalent to some of the earliest post-tessera plains units (for example, densely lineated plains, unit pdl; ridged and grooved plains, unit prg; Basilevsky and Head, 1995a, b) and that they started to form during this early period. In summary, volcanism at this time switched from the basin interior to the margins and from extensive floodlike plains units to digitate and lobate flows emanating from coronae along the basin margins, although the coronae had apparently started to form at the same time as earlier activity in the basin interior.

Of the several impact craters and splotches seen in the map area (fig. 1), we observed only one example of an impact crater possibly embayed by volcanic activity (unit pwr_1), and only one example of a crater possibly cut by tectonic activity. Thus, most impact craters appear to be younger than the regional plains. Rim heights of craters less than about 30 km in diameter should be <500 m in height (Sharpton, 1994). On the basis of the fact that no examples of craters embayed by pre-lobate plains units are observed and that the widespread deposits of wrinkle ridged plains material are thought to be relatively thin, we interpret the lack of embayed craters to indicate that the plains units were probably emplaced in a relatively short period, although the small total number of craters makes this interpretation very tentative.

In summary, the trends in the geologic history outlined here suggest that deformation decreased in intensity from an initially very high level associated with tessera formation, to increasingly lower levels associated with deformation of densely lineated plains, ridged and grooved plains, wrinkle ridged plains material, and, finally, to essentially no deformation of the latest flows of lobate plains. Trends in principle stress orientation suggest a relatively consistent post-tessera northwest-southeast principle compression axis orientation in the eastern part of the basin from early post-tessera through the emplacement of plains with wrinkle ridges. The topography of the basin in which Lavinia Planitia lies initially formed at the time of deformation of ridged and grooved plains (producing a series of smaller basins bounded by belts of units prg and bg) and continued to subside following partial filling of plains with wrinkle ridges. Volcanism was initially widespread and partly coincident with tessera formation (for example, units pdl and prg), then became concentrated into widely distributed small individual sources (the small shields of unit psh) in Lavinia Planitia, then changed style and was focused in the basin interior filling individual basins with possible large volume eruptions, and finally, changed style and location, erupting from coronae and related features along the basin margins into the basin interior where volcanism had apparently ceased.

Acknowledgments—We wish to thank Kari Magee, Susan Keddie, Martha Gilmore, and Aileen Yingst, who participated in early geologic mapping of the quadrangle, and Alexander Basilevsky and Jayne Aubele for detailed discussion about regional and global units and relations. We particularly appreciate the helpful discussions which occurred during the annual Venus Mappers' meetings and during an informal mapping workshop held at Brown University in the summer of 1995 and attended by George McGill, Steve Saunders, Jim Zimbelman, Alexander Basilevsky, Elizabeth Rosenberg, and Nathan Bridges. Their comments and discussions were most helpful in this effort. We also thank George McGill, Ronald Greeley, and Kelly Bender for helpful detailed map reviews. Financial support from the NASA Planetary Geology and Geophysics Program (Grant NAGW–5023) is gratefully acknowledged.

Table 1. *Physical property values for units in Lavinia Planitia quadrangle.*

[Note: Numbers in parentheses are minimum and maximum values; synthetic aperture radar (SAR) echo values were derived using mgn_data program, the remaining values were derived using anc_data program]

Unit	Latitude (° S.)	Longitude (° E.)	Incidence angle	SAR echo (decibels)	Elevation (kilometers)	Root mean square slope (degrees)	Fresnel reflectivity	Emissivity	Dielectric values Smooth	Dielectric values Rough
c	26.12	339.67	34.9	−8.936 (−13.221, −6.822)	6051.822 (6051.633, 6051.900)	3.47 (2.50, 4.80)	0.104 (0.085, 0.125)	0.832 (0.828, 0.835)	4.1	5.6
pl	34.39	354.76	30.3	−12.248 (−13.590, −11.224)	6051.048 (6051.027, 6051.083)	2.19 (1.40, 2.90)	0.100 (0.090, 0.110)	0.854 (0.853, 0.855)	3.9	4.9
ps	41.76	330.47	26.7	−17.068 (−18.609, −15.934)	6052.330 (6052.253, 6052.421)	2.73 (2.10, 3.10)	0.120 (0.115, 0.130)	0.818 (0.806, 0.824)	5.1	6.2
pwr_2	37.48	350.33	28.7	−11.805 (−13.070, −10.827)	6050.628 (6050.615, 6050.670)	2.28 (2.00, 2.50)	0.103 (0.095, 0.110)	0.859 (0.856, 0.862)	3.9	4.8
pwr_1	45.67	350.83	24.9	−10.828 (−11.840, −10.008)	6050.646 (6050.622, 6050.665)	1.76 (1.60, 2.00)	0.087 (0.075, 0.100)	0.877 (0.874, 0.880)	3.7	4.3
psh	49.21	342.88	23.6	−10.136 (−11.734, −8.971)	6050.698 (6050.654, 6050.754)	3.14 (1.50, 4.20)	0.079 (0.055, 0.085)	0.884 (0.883, 0.885)	3.6	4.1
bg	40.60	353.11	27.2	−6.567 (−12.463, −4.155)	6051.465 (6051.239, 6051.793)	4.77 (3.00, 6.30)	0.056 (0.050, 0.065)	0.902 (0.898, 0.905)	3.1	3.6
prg	46.63	341.89	24.5	−8.769 (−11.641, −7.055)	6050.490 (6050.101, 6050.625)	4.35 (2.90, 5.40)	0.081 (0.070, 0.095)	0.886 (0.881, 0.890)	3.5	4.1
pdl	25.91	353.41	35.0	−8.926 (−14.126, −6.626)	6051.549 (6051.131, 6051.648)	5.72 (4.70, 6.70)	0.134 (0.100, 0.180)	0.870 (0.868, 0.872)	3.3	4.4
t	23.65	358.92	36.2	−8.925 (−19.401, −6.114)	6053.442 (6052.870, 6053.935)	6.10 (4.10, 9.30)	0.071 (0.060, 0.095)	0.883 (0.874, 0.888)	3.0	4.1

Figure 1. Distribution of impact craters, splotches, coronae and coronaelike features, and volcanic edifices (steep-sided domes) in Lavinia Planitia quadrangle.

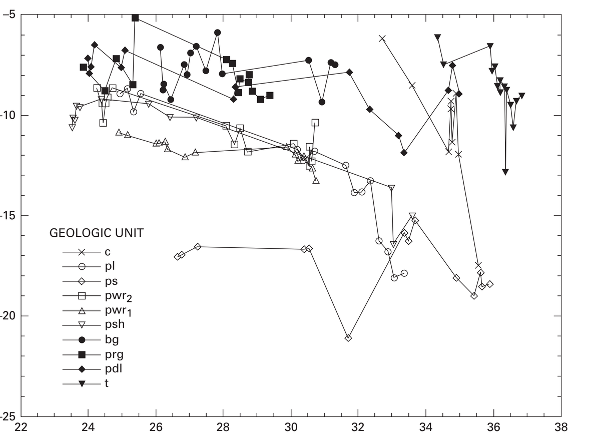

Figure 2. Diagram showing relation between incidence angle and backscatter coefficient for units in Lavinia Planitia quadrangle.

REFERENCES CITED

American Commission on Stratigraphic Nomenclature, 1961, Code of Stratigraphic Nomenclature: American Association of Petroleum Geologists Bulletin, v. 45, no. 5 p. 645–665.

Aubele, J.C., 1994, Stratigraphy of small volcanoes and plains terrain in Vellamo Planitia, Venus [abs.]: Lunar and Planetary Science Conference, 25th, Houston, Texas, March 14–18, 1994, Abstracts, p. 45–46.

———1995, Stratigraphy of small volcanoes and plains terrain in Vellamo Planitia–Shimti tessera region, Venus [abs.]: Lunar and Planetary Science Conference, 26th, Houston, Texas, March 13–17, 1994, Abstracts, p. 59–60.

Aubele, J.C., and Slyuta, E.N., 1990, Small domes on Venus—Characteristics and origin: Earth, Moon and Planets, v. 50/51, p. 493–532.

Baer, G., Schubert, G., Bindschadler, D.L., and Stofan, E. R., 1994, Spatial and temporal relations between coronae and extensional belts, northern Lada Terra, Venus: Journal of Geophysical Research, v. 99, p. 8355–8369.

Barsukov, V.L., and 29 others, 1986, The geology and geomorphology of the Venus surface as revealed by the radar images obtained by Veneras 15 and 16: Journal of Geophysical Research, v. 91, p. D378–D398.

Basilevsky, A.T., and Head, J.W., 1995a, Global stratigraphy of Venus—Analysis of a random sample of thirty-six test areas: Earth, Moon and Planets, v. 66, p. 285–336.

———1995b, Regional and global stratigraphy of Venus—A preliminary assessment and implications for the geologic history of Venus: Planetary Space Science, v. 43, p. 1523–1553.

———1996, Evidence for rapid and widespread emplacement of volcanic plains on Venus—Stratigraphic studies in the Baltis Vallis region: Geophysical Research Letters, v. 23, p. 1497–1500.

———1998, Onset time and duration of corona activity on Venus—Stratigraphy and history from photogeologic study of stereo images: Earth, Moon and Planets, v. 76, p. 67–115

Basilevsky, A.T., Head, J.W., Schaber, G.G., and Strom, R.G., 1997, The resurfacing history of Venus, *in* Phillips, R., and others, eds., Venus II: Tucson, University of Arizona Press, p. 1047–1084

Basilevsky, A.T., Nikolaeva, O.V., and Weitz, C.M., 1992, Geology of the Venera 8 landing site region from Magellan data—Morphological and geochemical considerations: Journal of Geophysical Research, v. 97, p. 16,315–16,335.

Basilevsky, A.T., Pronin, A.A., Ronca, L.B., Kryuchkov, V.P., Sukhanov, A.L., and Markov, M.S., 1986, Styles of tectonic deformations on Venus—Analysis of Venera 15 and 16 data: Journal of Geophysical Research, v. 91, p. D399–D411.

Bender, K.C., Senske, D.A., and Greeley, Ronald, 1999, Geologic map of the Carson quadrangle (V–43), Venus: U.S. Geological Survey Geologic Investigations Map 2620, scale 1:5 million, in press.

Bindschadler, D.L., Decharon, A., Beratan, K.K., Smrekar, S.E., and Head, J.W., 1992a, Magellan observations of Alpha Regio—Implications for formation of complex ridged terrains on Venus: Journal of Geophysical Research, v. 97, p. 13,563–13,578.

Bindschadler, D.L., and Head, J.W., 1991, Tessera terrain, Venus—Characterization and models for origin and evolution: Journal of Geophysical Research, v. 96, p. 5889–5907.

Bindschadler, D.L., Schubert, G., and Kaula, W.M., 1992b, Coldspots and hotspots—Global tectonic and mantle dynamics of Venus: Journal of Geophysical Research, v. 97, p. 13,495–13,532.

Campbell, B.A., 1995, Use and presentation of Magellan quantitative data in Venus mapping: U.S. Geological Survey Open-File Report 95–519, 32 p.

Campbell, D.B., Senske, D.A., Head, J.W., Hine, A.A., and Fisher, P.C., 1990, Venus southern hemisphere—Geologic characteristics and age of major terrains in the Themis–Alpha–Lada region: Science, v. 251, p. 180–183.

Campbell, D.B. Stacy, N.J.S., Newman, W.I., Arvidson, R.E., Jones, E.M., Musser, G.S., Roper, A.Y., and Schaller, C., 1992, Magellan observations of extended crater related features on the surface of Venus: Journal of Geophysical Research, v. 97, p. 16,249–16,277.

Crumpler, L.S., Head, J.W., and Aubele, J.C., 1993, Relation of major volcanic center concentration on Venus to global tectonic patterns: Science, v. 261, p. 591–595.

Elachi, C., 1987, Introduction to the physics and techniques of remote sensing: New York, Wiley and Sons, 413 p.

Ford, P.G., and Pettengill, G.H., 1992, Venus topography and kilometer-scale slopes: Journal of Geophysical Research, v. 97, p. 13,102–13,114.

Gilmore, M.S., and Head, J.W., 1992, Sequential deformation of plains along tessera boundaries on Venus—Evidence from Alpha Regio [abs.], *in* Abstracts of the International Colloquium on Venus, Pasadena, Calif., August 10–12, 1992: Lunar and Planetary Institute Contribution No. 789, p. 34–36.

Gilmore, M.S., Ivanov, M.A., Head, J.W., and Basilevsky, A.T., 1996, Deformation of craters on tessera terrain, Venus [abs]: Lunar and Planetary Science Conference, 27th, Houston, Texas, March 18–22, 1996, Abstracts, p. 419–420.

Greeley, R., Arvidson, R.E., Elachi, C., Geringer, M.A., Plaut, J.J., Saunders, R.S., Schubert, G., Stofan, E.R., Thouvenot, E.J.P., Wall, S.D., and Weitz, C.M., 1992, Aeolian features on Venus—Preliminary Magellan results: Journal of Geophysical Research, v. 97, p. 13,319–13,345.

Guest, J.E., Bulmer, M.H., Aubele, J., Beratan, K., Greeley, R., Head, J.W., Michaels, G., Weitz, C., and Wiles, C., 1992, Small volcanic edifices and volcanism in the plains of Venus: Journal of Geophysical Research, v. 97, p. 15,949–15,966.

Head, J.W., Crumpler, L.S., Aubele, J.C., Guest, J. E., and Saunders, R. S., 1992, Venus volcanism—Classification of volcanic features and structures, associations, and global distribution from Magellan data: Journal of Geophysical Research, v. 97, p. 13,153–13,197.

International Astronomical Union, 1999, Working Group for Planetary System Nomenclature, *in* Proceedings of the 23d General Assembly, Kyoto, Japan: Transactions of the International Astronomical Union, v. 23B, p. 247–248.

Ivanov, M.A., and Basilevsky, A.T., 1993, Density and morphology of impact craters of tessera terrain, Venus: Geophysical Research Letters, v. 20, p. 2579–2582.

Ivanov, M.A., and Head, J.W., 1996, Tessera terrain on Venus—A survey of the global distribution, characteristics, and relation to surrounding units: Journal of Geophysical Research—Planets, v. 101, p. 14,861–14,908.

———1998, Major issues in Venus geology—Insights from a global geotraverse at 30N latitude: Lunar and Planetary Science Conference, 29th, Houston, Texas, March 16–20, 1998, Abstract no. 1419.

Ivanov, B.A., Nemchinov, I.V., Svetsov, V.A., Provalov, A.A., Khazins, V.M. and Phillips, R.J., 1992, Impact cratering on Venus—Physical and mechanical models: Journal of Geophysical Research, v. 92, p. 16,167–16,181.

Keddie, S.T., and Head, J.W., 1995, Formation and evolution of volcanic edifices on the Dione Regio rise, Venus: Journal of Geophysical Research, v. 100, p. 11,729–11,754.

Konopliv, A.S., and Sjogren, W.L., 1994, Venus spherical harmonic gravity model to degree and order 60: Icarus, v. 112, p. 42–54.

Magee, K.P., and Head, J.W., 1995, The role of rifting in the generation of melt—Implications for the origin and evolution of the Lada Terra–Lavinia Planitia region of Venus: Journal of Geophysical Research—Planets, v. 100, p. 1527–1552.

Magee Roberts, K.M., Guest, J.E., Head, J.W., and Lancaster, M.G., 1992, Mylitta Fluctus, Venus—Rift-related, centralized volcanism and the emplacement of large-volume flow units: Journal of Geophysical Research, v. 97, p. 15,991–16,015.

Pavri, B., Head, J.W., Klose, K.B., and Wilson, L., 1992, Steep-sided domes on Venus—Characteristics, geologic setting, and eruption conditions from Magellan data: Journal of Geophysical Research, v. 97, p. 13,445–13,478.

Pettengill, G.H., Eliason, E., Ford, P.G., Loriot, G.B., Masursky, H., and McGill, G.E., 1980, Pioneer Venus radar results—Altimetry and surface properties: Journal of Geophysical Research, v. 85, p. 8261–8270.

Phillips, R.J., Raubertas, R.F., Arvidson, R.E., Sarkar, E.C., Herrick, R.R., Izenberg, N., and Grimm, R.E., 1992, Impact craters and Venus resurfacing history: Journal of Geophysical Research, v. 97, p. 15,923–15,948.

Saunders, R.S., and 26 others, 1992, Magellan mission summary: Journal of Geophysical Research, v. 97, p. 13,067–13,090.

Schaber, G.G., Strom, R.G., Moore, H.J., Soderblom, L.A., Kirk, R.L., Chadwick, D.J., Dawson, D.D., Gaddis, L.R., Boyce, J.M., and Russell, J., 1992, Geology and distribution of impact craters on Venus—What are they telling us?: Journal of Geophysical Research, v. 97, p. 13,257–13,302.

Schultz, P., 1992, Atmospheric effects on ejecta emplacement and crater formation on Venus from Magellan: Journal of Geophysical Research, v. 97, p. 183–248.

Scott, D.H., and Tanaka, K.L., 1986, Geologic map of the western equatorial region of Mars: U.S. Geological Survey Miscellaneous Investigations Series Map I–1802–A, scale 1:15,000,000.

Senske, D.A., Campbell, D.B., Stofan, E.R., Fisher, P.C., Head, J.W., Stacy, N., Aubele, J.C., Hine, A.A., and Harmon, J.K., 1991, Geology and tectonics of Beta Regio, Guinevere Planitia, Sedna Planitia, and western Eistla Regio, Venus—Results from Arecibo image data: Earth, Moon and Planets, v. 55, p. 163–214.

Sharpton, V.L., 1994, Evidence from Magellan for unexpectedly deep complex craters on Venus, *in* Dressler, B.O., Grieve, R.A.F., and Sharpton, V.L., eds., Large meteorite impacts and planetary evolution: Geological Society of America Special Paper 293, p. 19–27.

Solomon, S.C., Smrekar, S.E., Bindschadler, D.L., Grimm, R.E., Kaula, W.M., McGill, G.E., Phillips, R.J., Saunders, R.S., Schubert, G., Squyres, S.W., and Stofan, E.R., 1992, Venus tectonics—An overview of Magellan observations: Journal of Geophysical Research, v. 97, p. 13,199–13,256.

Squyres, S.W., Jankowski, D.G., Simons, M., Solomon, S.C., Hager, B.H., and McGill, G.E., 1992, Plains tectonism on Venus: The deformation belts of Lavinia Planitia: Journal of Geophysical Research, v. 97, p. 13,579–13,600.

Stofan, E.R., Sharpton, V.L., Schubert, G., Baer, G., Bindschadler, D.L., Janes, D.M., and Squyres, S.W., 1992, Global distribution and characteristics of coronae and related features on Venus: Implications for origin and relation to mantle processes: Journal of Geophysical Research, v. 94, p. 13,347–13,378.

Strom, R.G., Schaber, G.G., and Dawson, D.D., 1994, The global resurfacing of Venus: Journal of Geophysical Research, v. 99, p. 10,899–10,926.

Sukhanov, A.L., 1992, Tesserae, *in* Barsukov, V.L., Basilevsky, A.T., Volkov, V.P., and Zharkov, V.N., eds., Venus geology, geochemistry, and geophysics: Tucson, University of Arizona Press, p. 82–95.

Tanaka, K.L. (compiler), 1994, Venus geologic mappers' handbook, second edition: U.S. Geological Survey Open-File Report 94–438, 50 p.

Tyler, G.L., Simpson, R.A., Maurer, M.J., and Holmann, E., 1992, Scattering properties of the venusian surface—Preliminary results from Magellan: Journal of Geophysical Research, v. 97, p. 13,115–13,140.

Wilhelms, D.E., 1990, Geologic mapping, *in* Greeley, Ronald, and Batson, R.M., eds., Planetary mapping: New York, Cambridge University Press, p. 208–260.

ISBN 0-607-94505-2

Any use of trade, product, or firm names in this publication is for descriptive purposes only and does not imply endorsement by the U.S. Government

For sale by U.S. Geological Survey, Information Services, Box 25286, Federal Center, Denver, CO 80225, 1–888–ASK–USGS

Printed on recycled paper

GEOLOGIC MAP OF THE LAVINIA PLANITIA QUADRANGLE (V–55), VENUS

By
Mikhail A. Ivanov and James W. Head, III

2001